12 Dec 2016

The Shape of Water and Air Vortices

M. J. Germuska
Retired, 47 Clifden Road, Worminghall, HP18 9JR, UK.
mgermuska@aol.com, phone: +(44) 1844 339754

Abstract

This paper presents a new formula found experimentally for the shape of the free surface of stable vortices. It is a generalisation of the theoretical formula for the irrotational vortex in the ideal fluid. The new formula applies to real vortices where viscosity and compression may be present. The experiments were carried out under laboratory conditions on water and air vortices that were produced in several different ways.

Keywords: Fluid Dynamics, Vortices, Free Surface, Water, Air

1. Introduction

The shape of the free surface of the irrotational vortex in the ideal fluid is such that the square of the radius is inversely proportional to the depth (Kundu 2008) and may be given by formula (1.1).

$$r(z) = a\left(\frac{a}{z}\right)^{\frac{1}{2}} \qquad \text{where} \qquad a \succ 0 \tag{1.1}$$

The fluid is ideal if it is incompressible and has no viscosity. A vortex is said to be irrotational if the vorticity is zero everywhere, except for the singularity at the centre. Loosely speaking, a leaf on the surface of the irrotational vortex moves around the centre of the vortex but does not change its orientation, its stalk always points in the same direction, say to the north.

The formula applies also to viscose but incompressible fluids if the vortex boundaries are far enough from its centre, so that the friction at the boundaries is negligible, since in the absence of boundaries the net viscose force on an element vanishes everywhere (Kundu 2008). If the boundaries are not far enough or the fluid is compressible then the equations are too difficult to solve. The shape of the irrotational vortex is a theoretical limit far removed from real vortices, as will be shown here. Real vortices have the shape given by formula (1.2) which I will call Vir.

$$r(z) = a\left(\frac{a}{z}\right)^{\alpha} \qquad \text{where} \qquad \alpha \succ 0 \qquad a \succ 0 \tag{1.2}$$

Vir formula differs from formula (1.1) only in the values of the exponent α, which determines the shape of the vortex. The parameter a gives the size, when $z = a$ then $r = a$ and vice versa. For the vortices considered here $\alpha = [0.6, 2.5]$. The value 0.6 is for the vortex where the boundaries are far from the vortex centre. All vortices are in a stable state touching a solid surface at the narrow end, since during their rise and decay their shapes vary quickly and substantially.

Using regression we can say with the confidence of 99.999% that the vortices considered here do not have the shape of the irrotational vortex in the ideal fluid. They fit Vir formula very well, the error area (over-runs + under-runs) in comparison to Vir is about 2% when vortices are not quite smooth or steady, i.e. the water level or the mist volume visibly changes, otherwise it is < 1%.

The rest of this introduction outlines how the vortices are produced, their photographs are marked, the optical distortions are corrected and the values of the parameters α and a are computed. Three different methods are used to produce water vortices, namely by rotating a disk or a ring close to the bottom of the vessel, pumping or sucking water using two parallel tubes facing opposite directions, using two coupled water bottles. In order to produce vortices as stable as possible vibration must be reduced to a minimum. In the case of rotating disks and rings this is achieved by driving them using a wheel underneath the water container, with the connection provided by aligned pairs of magnets. In addition, a water-proof wheel-bearing houses the axis and screws with semi-spherical ends are fitted at the perimeter of the disk to act as stabilisers.

Air vortices are created from the mist produced by ultrasonic vibrations in water. The mist is fanned into a box of a square footprint and with a vertical slit in each corner. The slits are asymmetrical, offset in such a way that the air sucked into the box acquires angular momentum. The mist enters the box via a hole in the centre of the bottom where it hits a horizontal partition with smaller holes at the perimeter arranged in a circle. The mist rises through the holes and hits another horizontal partition, thus losing the upward linear momentum and spreading into an even layer. This partition has a large circular opening from which an upside down vortex emerges when the mist and air are sucked through a much smaller hole in the ceiling by the fan above. To produce a steady and dense vortex the suction must be as gentle as possible and the mist must have near ambient temperature. The speed of the fans has to be set very finely at the start, so that the volume of the mist in the box increases very gently, since any change afterwards disturbs the vortex and distorts its shape.

The photographs of vortices are marked by hand using a graphics software to trace the free surface. Markers are placed at regular intervals vertically or horizontally depending on the corresponding surface sections. The coordinates of the central pixel of the markers are recorded for further processing. To estimate the random human error in placing the markers five people marked the same photo of a water vortex and the standard deviation of the resulting errors was found. Real vortices are never perfectly symmetrical or vertical even if they are in a reasonably steady state. Thus a computer routine is used to combine the left arm and the mirror image of the right arm of the vortex into two symmetrical arms. The corresponding marks on the left and the right arm are then considered as the diameter of the disk at the given height of the vortex.

The diameter of a sphere is distorted on photographs, therefore another routine is used to correct this. Yet another routine is used to correct the distortion due to the light refraction on the boundary between air and water. Photographs, being two-dimensional projections of three-dimensional objects, distort shapes in other ways than mentioned above. Therefore a three dimensional solid model of the irrotational vortex in the ideal fluid was machined and photos of it taken with the camera at various elevations and angles. It was found that as long as the elevations and the angles are within certain limits then the distortions do not affect the accuracy of Vir formula, nor the value of the exponent alpha. However, for some elevations and angles close to those limits some rules about marking the free surface on the photographs have to be observed.

The coordinates of the corrected markers are used to find the parameters α and a that give the least sum of the squared errors. The computer routine that finds these parameters uses suitable ranges of both α and a as well as a suitable number of discrete points within these ranges. For each discrete pair (α, a) the fit error is computed and the pair with the minimum error is chosen. This is repeated using smaller ranges of the values until the desired accuracy is reached.

2. Processing the Photographs of Vortices

Real vortices are never perfectly vertical or perfectly symmetrical. A scheme for marking the vortex arms on the photographs was designed to deal with that. Using a graphics software photographs were sized to fit the vortex into a window of 400x400 to 500x500 pixels. A grid of 1 pixel thick lines, 5 pixels apart was superimposed on the photograph and markers of 3x3 pixels were manually placed along the edge of the vortex at intervals of 10 or 20 pixels, vertically and horizontally as appropriate. One arm and the mirror image of the other were used to produce the average arm, shown in figure 1, where the dashed line is the mirror image and the dotted line the average. The mirror image of the average arm gives us two symmetrical arms, in figure 2.

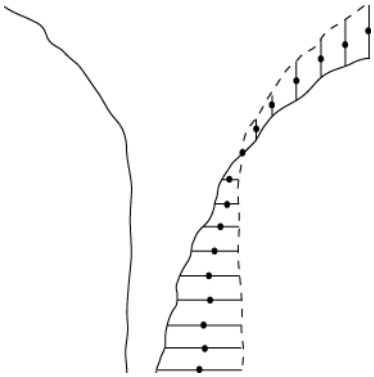

FIGURE 1. Combining vortex arms

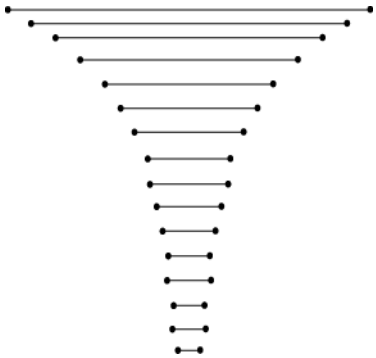

FIGURE 2. Vortex with symmetric arms

In figure 3 the horizontal line at the top of the diagram represents the diameter of a disk or a cylinder. It is optically distorted and on a photograph appears greater than it is in reality. The light ray to the camera that is at the distance y_0 from the centre of a cylinder touches the cylinder at a tangent and has a greater angle α than the line from the camera to the extreme point x of the cylinder. Using similar triangles with the same angle α we find the formula (2.1) for correcting this distortion. The formula is only approximate because it does not involve the elevation and the angle of the camera, however it turns out that this is sufficient for our needs.

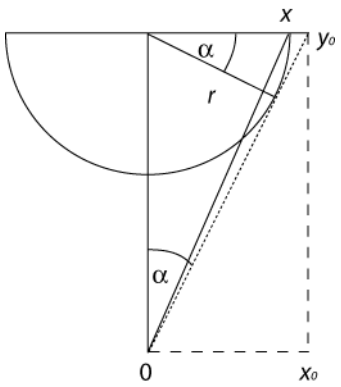

FIGURE 3. Tangential distortion

x_0 = apparent radius $\qquad r = x = \dfrac{x_0 y_0}{\sqrt{x_0^{\,2} + y_0^{\,2}}} \qquad$ y_0 = camera distance $\qquad$ (2.1)

Another optical distortion is due to the refraction of light at the boundary between air and water. The refraction formula was first found by Snell (1591-1626), expressed using cosecants of the angles. These days we use mostly the sins formula due to Descartes (1596-1650), where n stands for the refractive index and α for the incident angle (Meyer-Arendt 1972).

$$n_1 \sin(\alpha_1) = n_2 \sin(\alpha_2) \tag{2.2}$$

The refractive index n for some common media are: vacuum = 1, air = 1.0003, water = 4/3, spectacle glass C1 = 1.5230. These values are for the helium d line 587.6 and they vary with the wave length. If the boundary between the media is a plane we have the diagram in figure 4 below

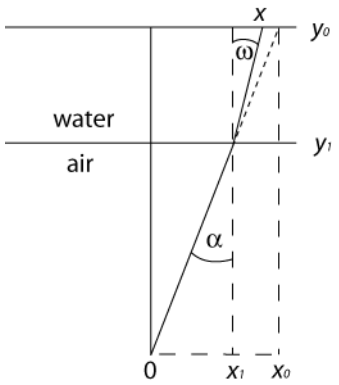

FIGURE 4. Refraction at a plane

If we place the camera at the origin of the coordinates then for the angles α and ω we have

$$\sin(\alpha) = \frac{x_0}{\sqrt{{x_0}^2 + {y_0}^2}} \qquad \sin(\omega) = \frac{x - x_1}{\sqrt{(x - x_1)^2 + (y - y_1)^2}} \tag{2.3}$$

Using Descartes formula with n representing the refractive index of water we get

$$\frac{x_0}{\sqrt{{x_0}^2 + {y_0}^2}} = n \frac{x - x_1}{\sqrt{(x - x_1)^2 + (y - y_1)^2}} \tag{2.4}$$

This leads to the formula for the actual distance of the point *x*, that appears on a photograph as x_0

$$x = x_0 \left(\frac{y_1}{y_0} + \frac{y_0 - y_1}{\sqrt{(n^2 - 1){x_0}^2 + n^2 {y_0}^2}} \right) \tag{2.5}$$

This formula is used to correct the refraction distortion when a vortex is produced in a laboratory using a square container. It is assumed that the transparent walls are thin in comparison to the size of the container and hence the diffraction due to the walls can be neglected. The profile of the vortex, the wall and the lens are all in parallel planes. Thus the distance *x* may stand either for the radius or the depth of the vortex, both of them may be corrected using the above formula.

When a cylindrical container is used then the situation is more complicated, as shown in figure 5.

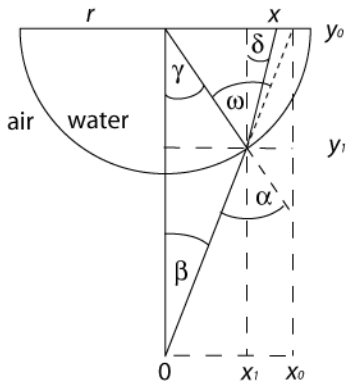

FIGURE 5. Refraction at a cylinder

We can no longer find a simple formula, instead we find several formulas that can be used in sequence to correct the distortion. Using the similar triangles with the common angle β we get

$$x_1 = x_0 \frac{y_1}{y_0} \qquad r = \sqrt{\left(x_0 \frac{y_1}{y_0}\right)^2 + (y_0 - y_1)^2} \tag{2.6}$$

From the above we get the quadratic equation shown below for the unknown y_1

$$y_1 = \frac{B - \sqrt{B^2 - 4AC}}{2A} \tag{2.7a}$$

where $$A = \left(\frac{x_0}{y_0}\right)^2 + 1 \qquad B = 2y_0 \qquad C = {y_0}^2 - r^2 \tag{2.7b}$$

The angles α, β, γ, δ and ω can be obtained directly from the diagram and they are given below

$$\beta = \tan^{-1}\left(\frac{x_0}{y_0}\right) \qquad \gamma = \tan^{-1}\left(\frac{x_1}{y_0 - y_1}\right) \tag{2.8}$$

$$\alpha = \beta + \gamma \qquad \omega = \sin^{-1}\left(\frac{1}{n}\sin(\alpha)\right) \qquad \delta = \omega - \gamma \tag{2.9}$$

$$x = x_1 \frac{y_1}{y_0} + (y_0 - y_1)\tan(\delta) \tag{2.10}$$

Using a cylinder there is also vertical refraction that can be treated as the refraction in a plane, provided that the level of the camera is close to the top of the vortex. This is because in such circumstances there is little vertical refraction at the top of the vortex and the vertical part of the vortex is so narrow that in that range the surface of the cylinder can be considered flat.

3. Fitting Vir to Vortex

When we have some data and a function $y(x)$ the usual procedure to find the parameters of the function $y(x)$ with the best fit to the data is to minimize the sum of the squared errors Δy^2. The problem with this method is that it gives different parameters for r =Vir(z) and for z = Vir^{-1}(r), i.e. when the axes are swapped. This is because the errors on the vertical section dominate the errors on the horizontal. The outcome should be independent of the coordinate system that happens to be used. We achieve this by using the distance Δh of the point from the curve, shown in figure 6.

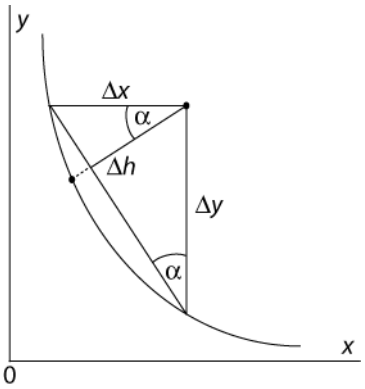

FIGURE 6. Distance from a Curve

Using similar right-angle triangles we obtain the formula for Δh and the standard deviation σ

$$\Delta h = \frac{\Delta x \Delta y}{\sqrt{\Delta x^2 + \Delta y^2}} \qquad \sigma = \sqrt{\frac{\Sigma \Delta h^2}{N-1}} \tag{3.1}$$

Vir can be fitted to the data by choosing suitable ranges for the parameters α and a, the number of discrete points in these ranges and then use a routine that finds the pair (α, a) with the minimum sum of squared errors. Instead of parameter a one can use the distance between the top of the vortex and the level of Vir at infinite radius. This is easier to visualise and hence this method is used. If need be, one of the marker points may be chosen as the "Anchor" with zero error. Throughout this paper all Vir exponents α are calculated with the precision of plus-minus 0.001.

The fit error σ thus obtained is given in pixels which is easy to understand, but it is not a consistent measure for all vortices, because it depends on the size of the photograph and the corrections of distortions. Thus we define dimension-less quantities ρ, ζ and write Vir function (1.2) as in (3.2)

$$\rho = \ln\left(\frac{r}{a}\right) \qquad \zeta = -\ln\left(\frac{z}{a}\right) \qquad \text{thus} \qquad \rho = \alpha\zeta \tag{3.2}$$

Quantities ρ and ζ are used for linear regression with the intercept set to zero, since $\rho(0) = 0$. Regression parameters "R Square", "P Value" and "Standard Error" are recorded for each vortex examined, as indicators of the goodness of fit. To estimate the accuracy of α the Confidence Range of 95% and 99.999% are also recorded.

4. Precision of the Method

Throughout this paper the photographs shown are reduced to 220x220 pixels with enlarged markers for better visibility. To estimate the precision of the method employed a computer was used to print the outline of a 14x14 cm irrotational vortex in the ideal fluid. The printout was used to cut a template from a stiff sheet of paper for producing a 3D model on a wood lathe. Figure 7 shows a photo of the template. The coordinates of the markers were used to find the fit errors to Vir with $\alpha = ½$. A standard routine was then used to calculate the linear regression parameters (3.2), including the Line Fit Plot shown in figure 8.

FIGURE 7. Template, $\alpha = 1/2$, $\sigma = 0.41$ pix

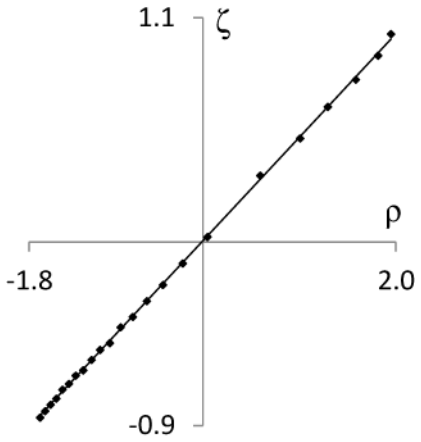

FIGURE 8. Template, $R^2 = 0.9998$, P = E-41

FIGURE 9. Profile, $\alpha = 1/2$, $\sigma = 0.58$ pix

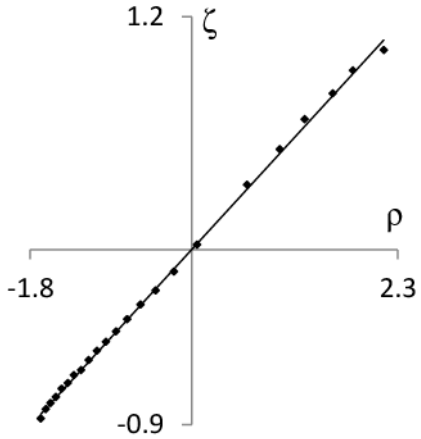

FIGURE 10. Profile, $R^2 = 0.9989$, P = E-34

The profile of the 3D model in figure 9 was obtained by using a carpenter's square, a scalpel and a sheet of paper. The model is quite true to the template, except for the last 5 mm at the edge, where it deviates by about 0.5 - 1 mm. The profile is not as accurate as the template, as can be seen in figure 10, the standard deviations $\sigma = 0.41$, 0.58 pix, as well as the regression errors $\pm\Delta\alpha = 0.003$, 0.007 at 95% confidence. Other regression parameters are $R^2 = 0.9998$, 0.9989 and P = E-41, E-34.

The photo in figure 7 of the two-dimensional template does not suffer from any optical distortions that 3D objects suffer. It shows the vortex boundaries that follow a printed outline of a Vir with the known α and a. Thus the fit error $\sigma = 0.41$ pix is entirely due to the random human inconsistency in placing the markers. Since this photo is clearer than any photo of the real vortices that are presented in this paper the lower limit of the random human error contribution to σ is 0.41 pix.

To estimate the upper limit of this error five people marked a photo of a water vortex that was of poorer quality than any of the example vortices, because the water was not very clear. One person marking the photo was partly colour-blind to red and another to blue. Fifteen marks were placed on both the left arm and the right arm of the vortex, thus the marking process generated 150 errors. Using the standard deviation of these errors it was found that the upper limit of the human error contribution to σ is 0.92 pix.

Thus for the example vortices in this paper the human error contribution is estimated to be the average of the above mentioned minimum and maximum, i.e. the contribution to σ is 0.66 pix.

The vortex fit parameter σ is measured in pixels and hence it is easy to visualise, but it is not very good for comparing the goodness of fit, because the photographs are not all of the same size and those that are have different size vortices. However, using distances Δh (3.1) of the individual vortex markers from the Vir curve one can obtain an objective measure of the fit that can be used for comparing different example vortices. For this purpose we define the Error Area.

$$\text{Error Area} = (\text{union} - \text{intersection}) \text{ of the vortex and Vir profiles} \tag{4.1}$$

The Error Area can be closely approximated by the narrow strip enclosed by the line of straight segments connecting the vortex markers and the line of the corresponding straight segments on the Vir. This approximation of the Error Area can easily be computed at the same time as the standard deviation σ. The Vir Area is computed using the integral of the Vir.

$$\text{Vir Area} = \frac{a^2}{1-\alpha}\left[\left(\frac{z2}{a}\right)^{1-\alpha} - \left(\frac{z1}{a}\right)^{1-\alpha}\right] \quad \text{for } \alpha \neq 1 \qquad \text{and} \qquad a^2 \cdot \ln\left(\frac{z2}{z1}\right) \quad \text{for } \alpha = 1 \tag{4.2}$$

The ratio of the two areas gives us the Relative Area Error (RAE) which is an objective measure for quantifying and comparing the goodness of fit.

$$\text{RAE} = \text{Error Area}/\text{Vir Area} \tag{4.3}$$

For the template in figure 7 we have REA = 0.005, which is all due to the human error in marking. We found above that the human error contribution to σ is 0.41 pix for the template and 0.66 pix for real vortices. i.e. approximately in the ratio 2:3. Thus if all Vir Areas were the same as for the template then the contribution of the human error to REA would increase proportionally from 0.005 to 0.0075. It turns out that the Vir Area for the example vortices is always less than for the template and thus the contribution of the human error to RAE is always greater than 0.0075.

$$\text{For real vortices the minimum contribution of human error to RAE} = 0.0075 \tag{4.4}$$

If we subtract the above value in (4.4) from RAE for the example vortices we get the RAE values that would be obtained in the absence of the random human errors.

5. Solid Model of Irrotational Vortex

In addition to the distortions already considered, the photographs can be distorted due to the level and the angle of the camera. To find this distortion and the ways of preventing or correcting it photographs of the solid model of the irrotational vortex were used. When the camera is at an angle greater than 15 degrees then the photos become too distorted, the simple tangential correction (2.1) is insufficient and we get $\alpha < 0.45$. The photos of such examples are not shown. However, when the angle is less than 5 degrees and the camera is level or just below the top of the model then the error in α is quite small, as in the case of figures 11 and 12. In this case the top of the model is a bit distorted, because the camera was a bit too much below the level of the top.

FIGURE 11. Model A, $\alpha = 1/2$, $\sigma = 1.15$ pix

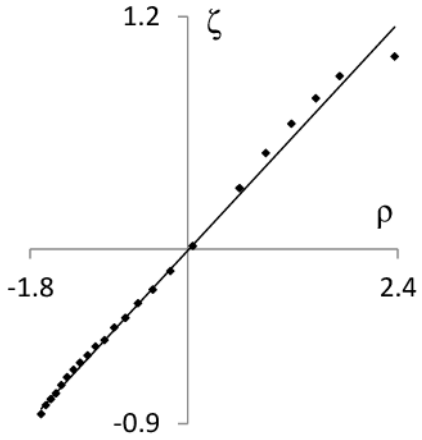

FIGURE 12. Model A, $R^2 = 0.9944$, P = E-26

FIGURE 13. Model B, $\alpha = 1/2$, $\sigma = 0.61$ pix

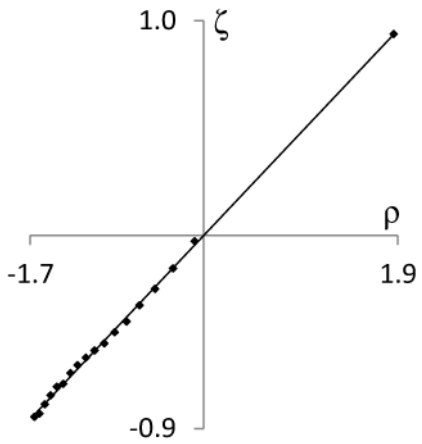

FIGURE 14. Model B, $R^2 = 0.9996$, P = E-30

The camera may also be at the bottom of the model, as in the case of figures 13, 14. In this case only the extreme horizontal marker, which must be placed with precision, is used. It is used as the "Anchor", i.e. the Vir curve is forced to go through it. The regression errors $\pm\Delta\alpha = 0.016, 0.005$ at 95% confidence. Other regression parameters are $R^2 = 0.9944, 0.9996$ and P = E-26, E-30.

6. Examples of Water Vortices

Three methods are used to produce water vortices, by rotating a disk or a ring at the bottom of the vessel, pumping water using two parallel tubes facing opposite directions, using coupled water bottles. Figures 15, 16 relate to a vortex produced by rotating a double ring with the diameter of 4cm, hole diameter 1cm and the ring thickness 3mm. The vortex is in a square 50cm container with the water level at 10 cm. The walls are thus far enough to create little friction and the vortex is close to the ideal irrotational model, which corresponds to the Vir with exponent $\alpha = ½$.

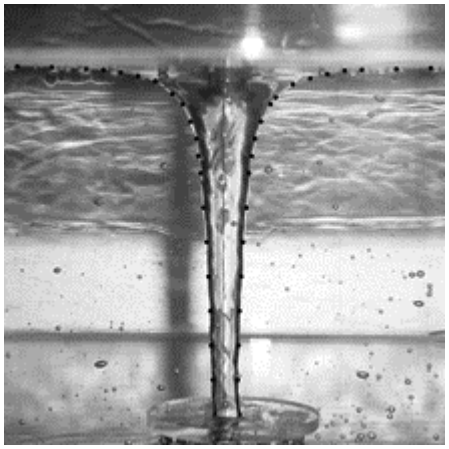

FIGURE 15. Ring, $\alpha = 0.60$, $\sigma = 0.52$ pix

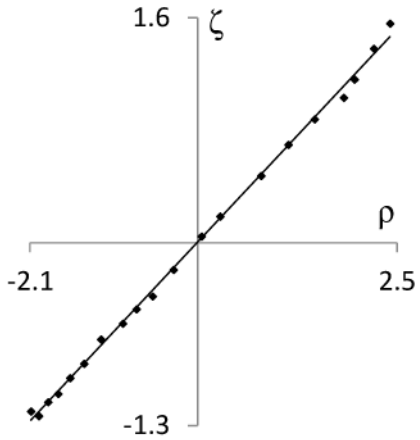

FIGURE 16. Ring, $R^2 = 0.9983$, P = E-28

FIGURE 17. Jets, $\alpha = 0.67$, $\sigma = 0.39$ pix

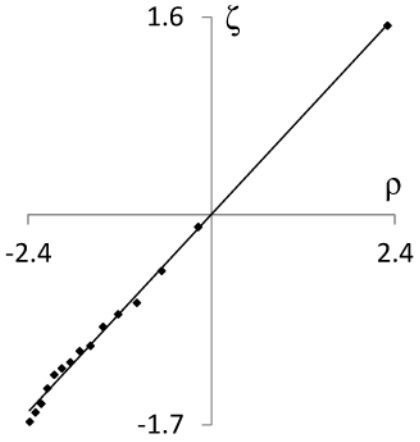

FIGURE 18. Jets, $R^2 = 0.9984$, P = E-21

Figures 17, 18 relate to a vortex at Seaham Hall, Sunderland, UK (Pye 2000) produced by pumping water using two parallel jets facing each other. It operates in three cycles, with the water filling, overflowing and draining away. When the water is overflowing at a steady rate the vortex is quite stable for about a minute, during which period the photo was taken. The cylinder is large, its diameter is 2.2m and height 2.3m. There is enough difference in the angular velocity at the bottom and the top to cause a screw-like shape of the vortex. For the two examples the errors $\pm\Delta\alpha = 0.012$, 0.015 at 95% confidence. Other parameters are $R^2 = 0.9983$, 0.9984 and P = E-28, E-21.

Figures 19, 20 relate to a vortex produced using two plastic one litre water bottles that are joined at their necks, filled with a bit less than one litre of water in all. The water is given some angular momentum by a circular movement using hands and then the bottles are placed in a holder to keep them steady. The flow of water is restricted by inserting a ring with the hole of 1cm in diameter where the bottles are joined. This makes the vortex last a bit longer, about 30 seconds.

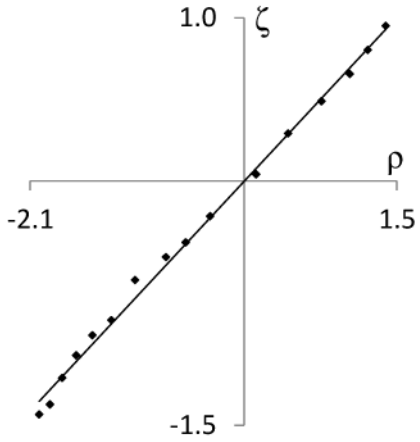

FIGURE 19. Bottles A, $\alpha = 0.65$, $\sigma = 1.04$ pix FIGURE 20. Bottles A, $R^2 = 0.9965$, P = E-20

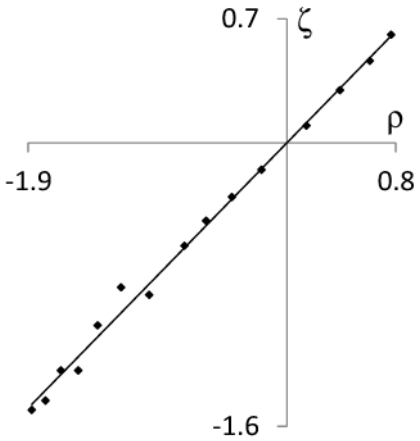

FIGURE 21. Bottles B, $\alpha = 0.77$, $\sigma = 1.25$ pix FIGURE 22. Bottles B, $R^2 = 0.9964$, P = E-18

Figures 21, 22 relate to a vortex taken at almost the same water level, but three minutes before the previous example above. The water level visibly decreases thus the vortices are semi-stable. However, they are not in the process of rising or decaying and hence satisfy the Vir formula quite well. The value of α depends mainly on the initial momentum. The difference of the angular velocities at the bottom and at the top results in a screw-like shape of the vortex vertical part, which affects figure 22 more than figure 20. For the two examples the errors $\pm\Delta\alpha = 0.022, 0.027$ at 95% confidence. Other regression parameters are $R^2 = 0.9965, 0.9964$ and P = E-20, E-18.

Figures 23, 24 relate to a vortex produced by rotating a disk close the bottom of the cylinder. The disk doesn't have a hole at its centre and without it the air cannot circulate so that we cannot see any bubbles rising, which are seen in figure 15. The height of the cylinder is 20cm, the inner diameter at the top is 11cm and at the bottom 10cm. Figures 25, 26 relate to another such vortex, with the cylinder height 15cm, the inner diameter at the top 14.5cm and at the bottom 13.5cm.

FIGURE 23. Disk A, $\alpha = 0.89$, $\sigma = 0.82$ pix

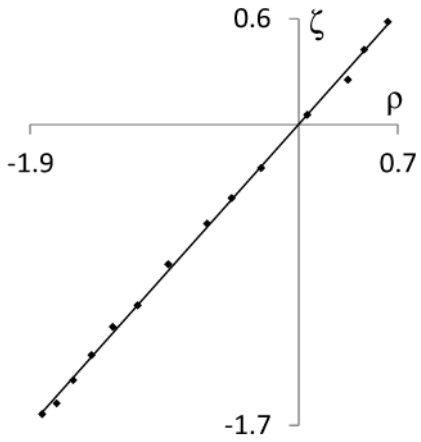

FIGURE 24. Disk A, $R^2 = 0.9993$, P = E-22

FIGURE 25. Disk B, $\alpha = 2.49$, $\sigma = 0.81$ pix

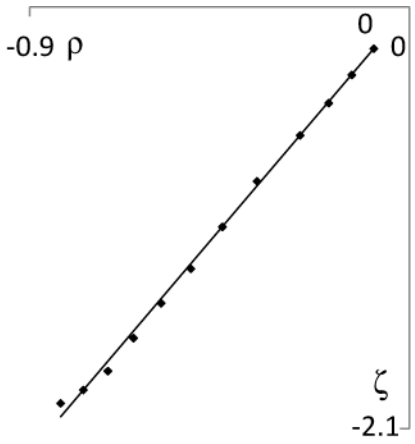

FIGURE 26. Disk B, $R^2 = 0.9995$, P = E-19

In both cases the gap between the disk and the wall is only about 1mm, hence there is more friction at the wall than in the previous examples resulting in the higher values of α. There is no screw effect in figure 25, possibly because the cylinder is low and hence the difference between the angular velocities at the bottom and the top is small. The plot in figure 26 is in the negative quadrant of the coordinates. This is because all values of *z*, *r* are smaller than the Vir parameter *a*, which is a bit greater than the radius of the cylinder. The origin of the coordinates is level with the Vir at infinity, which is about distance *a* above the top marker. The regression parameters for the two examples are $\pm\Delta\alpha = 0.014, 0.036$ at 95% confidence, $R^2 = 0.9993, 0.9995$ and P = E-22, E-19.

7. Examples of Air Vortices

Air vortices are created from the mist produced by ultrasonic vibrations in water. The mist is pumped into the bottom of the box and sucked out through the ceiling. The box has a square footprint 40x40cm, is 30cm high and has 1cm wide vertical slits in each corner. The slits are asymmetrical, offset in a way that the air sucked into the box acquires angular momentum. The circular hole in the bottom has a diameter of 30cm and in the ceiling 4cm. The speed of the fans pumping the mist in and sucking it out has to be set at the start, so that the volume of mist in the box increases very gently, since any change afterwards disturbs the vortex and distorts it shape. Figures 27, 28 relate to one such vortex, figures 29, 30 to another taken two minutes earlier.

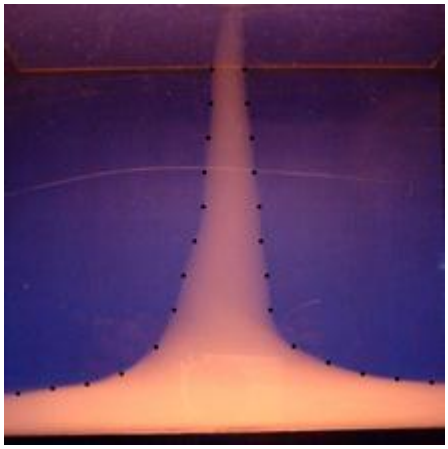

FIGURE 27. Mist A, $\alpha = 0.75$, $\sigma = 1.70$ pix

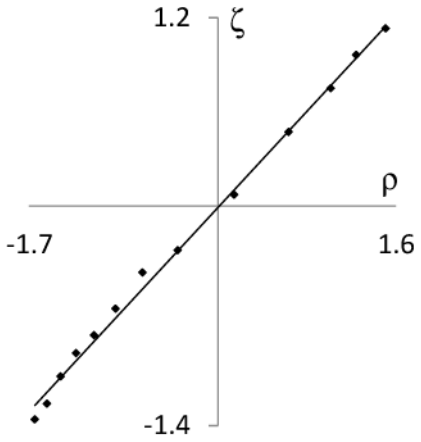

FIGURE 28. Disk A, $R^2 = 0.9966$, P = E-16

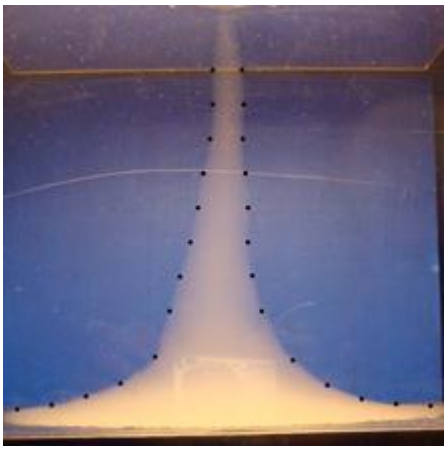

FIGURE 29. Mist B, $\alpha = 0.98$, $\sigma = 1.53$ pix

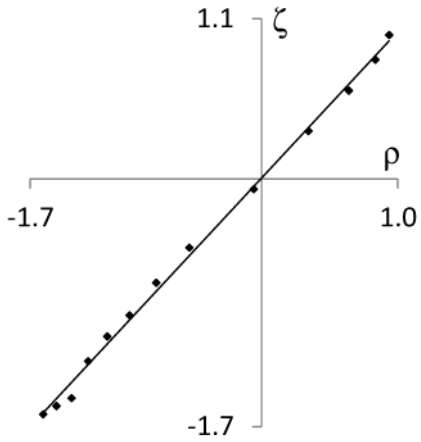

FIGURE 30. Disk B, $R^2 = 0.9978$, P = E-17

Because the volume of the mist in the box always visibly increases the vortices are semi-stable, slowly changing their shape all the time. However, they are not rising or decaying and the small end touches the ceiling, therefore they satisfy the Vir formula quite well. The errors $\pm\Delta\alpha = 0.028$, 0.030 at 95% confidence. Other regression parameters are $R^2 = 0.9966$, 0.9978 and P = E-16, E-17.

8. Regression Analysis

The parameters for the linear regression $\rho = \alpha\zeta$ (3.2) with zero intercept are shown in table 1.

Figure	Vortex Name	α Value	$\pm\Delta\alpha$ @95%	$\%\Delta\alpha/\alpha$ @95%	$\pm\Delta\alpha$ 99.999%	R Square	P Value	Points Used	STD Error
Fig. 7	Template	1/2	0.003	0.60%	0.010	0.9998	E-41	23	0.010
Fig. 9	Profile	1/2	0.007	1.40%	0.020	0.9989	E-34	23	0.021
Fig. 11	Model A	1/2	0.016	3.20%	0.045	0.9944	E-26	23	0.047
Fig. 13	Model B	1/2	0.005	1.00%	0.016	0.9996	E-30	18	0.013
Fig. 15	Ring	0.60	0.012	2.00%	0.034	0.9983	E-28	20	0.038
Fig. 17	Jets	0.67	0.015	2.24%	0.048	0.9984	E-21	15	0.049
Fig. 19	Bottles A	0.65	0.022	3.38%	0.067	0.9965	E-20	16	0.051
Fig. 21	Bottles B	0.77	0.027	3.51%	0.085	0.9964	E-18	15	0.054
Fig. 23	Disk A	0.89	0.014	1.57%	0.046	0.9993	E-22	14	0.027
Fig. 25	Disk B	2.49	0.036	1.45%	0.126	0.9995	E-19	12	0.030
Fig. 27	Mist A	0.75	0.028	3.73%	0.094	0.9966	E-16	13	0.053
Fig. 29	Mist B	0.98	0.030	3.06%	0.099	0.9978	E-17	13	0.050

TABLE 1. Regression Parameters

The first four rows in the table refer to the model of the irritational vortex which has $\alpha = ½$. For the template the error $\pm\Delta\alpha$ is 0.003 at 95% confidence and the other regression parameters show that the method used provides high precision. For the examples of the real vortices the error $\pm\Delta\alpha$ is from 0.012 to 0.036 at 95% confidence, with the corresponding values of $\alpha = (0.60, 2.49)$.

For each real vortex the value of $\alpha = ½$ is rejected with 99.999% confidence. Figure 31 shows two regression line plots for the vortex in figure 15, that has the smallest best fit $\alpha = 0.60$ of all examples. The first plot is for the best fit $\alpha = 0.60$ and the second for the forced $\alpha = ½$. This visually demonstrates the meaning of 99.999% confidence.

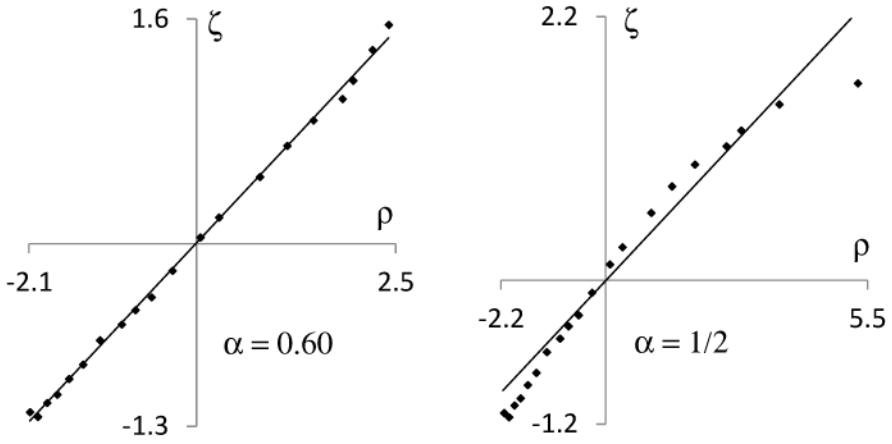

FIGURE 31. Regression Line Fit Plots for the vortex in figure 15, for $\alpha = 0.60$ and $\alpha = ½$

9. Vir Parameters Analysis

The Vir parameters (1.2) and the parameters indicating the goodness of fit are shown in table 2.

Figure	Vortex Name	α Value	*a* Value	Min z	Max z	Vir Area	Error Area	RAE	Points Used	Error σ pix
Fig. 7	Template	1/2	72.0	9.5	400.6	20662	107	0.005	23	0.412
Fig. 9	Profile	1/2	71.7	7.7	409.0	21164	180	0.008	23	0.578
Fig. 11	Model A	1/2	73.1	6.6	407.0	22012	351	0.016	23	1.149
Fig. 13	Model B	1/2	76.6	11.7	413.5	22696	235	0.010	18	0.606
Fig. 15	Ring	0.60	41.7	3.7	304.5	7981	106	0.013	20	0.521
Fig. 17	Jets	0.67	26.1	2.6	324.5	3782	102	0.027	15	0.392
Fig. 19	Bottles A	0.65	50.1	12.4	448.9	11037	327	0.030	16	1.042
Fig. 21	Bottles B	0.77	60.9	28.4	427.7	11688	318	0.027	15	1.251
Fig. 23	Disk A	0.89	63.3	33.7	398.5	10627	157	0.015	14	0.825
Fig. 25	Disk B	2.49	154.6	168.0	343.0	9243	107	0.012	12	0.809
Fig. 27	Mist A	0.75	74.1	16.5	454.7	19498	632	0.032	13	1.700
Fig. 29	Mist B	0.98	85.7	33.6	442.8	19033	503	0.026	13	1.530

TABLE 2. Vir Parameters

The vertical part of the vortex in figure 17 is like a screw while the vortices in figures 19, 21, 27, 29 are semi-stable because the water level is decreasing or the mist volume is increasing, hence their RAE is at the high end. If we exclude the random human errors RAE = 0.75% (4.4) for these vortices we get approximately RAE = 2%. For the more stable vortices in figures 15, 23, 25 we get RAE < 1%, which is of the same order as for the irrotational vortex model in figures 11, 13.

Figure 32 shows the Vir graphs of the vortices involved. Only six vortices are included, because the remaining have α very close to some already present and their inclusion would result in a smudge. All vortices have $a = 1$, since otherwise the comparison would be difficult. This is achieved by dividing the values of z and r by a. The bold curve, the highest on the plot, is for the ideal irrotational vortex with $\alpha = ½$, the lowest curve has $\alpha = 2.49$.

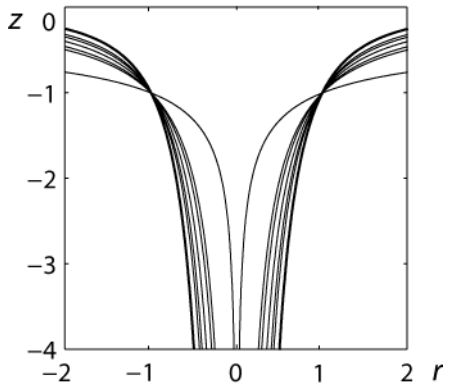

FIGURE 32. Vir graphs for the example vortices

10. Summary and Conclusions

1. Using regression we can say with the confidence of 99.999% that real vortices do not have the shape of the irrotational vortex in the ideal fluid.

2. The shape of steady vortices in water and air is given by the Vir formula, where the exponent α determines the shape and the parameter *a* the size. For the example vortices in this paper the range of the exponent α = [0.60, 2.49] while for the irrotational vortex in the ideal fluid α = ½.

$$\text{Vir\_}r(z) = a\left(\frac{a}{z}\right)^{\alpha} \qquad \text{where} \qquad \alpha \succ 0 \qquad a \succ 0$$

3. To quantify the goodness of fit of vortices to Vir we use the Relative Error Area (REA) which is the fraction Error Area/Vir Area. The Error Area consists of Vir over-run and under-run areas.

4. The vortex in figure 17 has a screw-like profile resulting from a large difference of the angular velocities at the bottom and the top of the vortex. It has REA of about 2%.

5. Vortices that are semi-stable, due to changing water level or mist volume at a rate that can easily be visually detected, as in figures 19, 21 and 27, 29 also have REA of about 2%.

6. Stable vortices in figures 15, 23, 25, where the water level or the mist volume does not change, have REA < 1%.

7. The random human errors in marking the vortex profile on the photographs of the example vortices contribute to RAE by 0.75%. This error is not included in the RAE fit errors given above.

8. The Vir formula does not apply to vortices during their rise and decay, i.e. during the stage when their shape is changing rapidly and substantially.

9. The Vir formula also does not apply to vortices that end in a sharp point instead of reaching a solid surface with the narrow end, even if they are reasonably steady.

10. From the above we conclude that the Vir formula should apply to tornados and hurricanes which touch the ground. However, this has not been verified since the author was unable to find photographs where the upper parts were not obscured by the foreground or background clouds.

11. If a way could be found of determining the Vir parameters for tornados and hurricanes then one could calculate their volume, mass and moments of inertia more precisely.

12. It may be possible to adapt the Euler equations of motion for solid spinning tops in fluids to work out the trajectories and energies of tornados and hurricanes more precisely.

13. It will be shown shortly in the paper entitled "Shapes with the Minimum Moment of Inertia" that the solid of rotation generated by the Vir function has the minimum moment of inertia of all concave spinning tops, i.e. that vortices give least resistance to spinning.

Acknowledgements

My thanks go William Pye, designer of the vortex Charybdis for permission to use the photograph in figure 17. Also to Richard Lyon for making the wood model of the irrotational vortex shown in figures 11, 13 and to Andy Bradley for machining metal parts used to generate the water vortices.

I would like to thank my wife Jo for her loving care without which this work would not have been possible. I thank God for everything.

References

Kundu, P. K. and Cohen, I. M. 2008 *Fluid Mechanics* (Academic Press) p.142,143,147

Meyer-Arendt, J. R. 1972 *Introduction to Classical and Modern Optics* (Prentice-Hall) p.14-16

Pye, W. 2000 http://www.williampye.com/work/charybdis